

Excitation Energy Transfer between the B850 and B875 Antenna Complexes of *Rhodobacter sphaeroides*[†]

V. Nagarajan* and W. W. Parson

Department of Biochemistry, Box 357350, University of Washington, Seattle, Washington 98195

Received October 9, 1996; Revised Manuscript Received December 20, 1996[®]

ABSTRACT: Energy transfer between the B850 (LH2) and B875 (LH1) antenna complexes of a mutant strain of *Rhodobacter sphaeroides* lacking reaction centers is investigated by femtosecond pump-probe spectroscopy at room temperature. Measurements are made at wavelengths between 810 and 910 nm at times extending to 200 ps after selective excitation of either B850 or B875. Assignments of the spectroscopic signals to the two types of antenna complex are made on the basis of measurements in strains that lack either LH1 or LH2 in addition to reaction centers. Energy transfer from excited B850 to B875 proceeds with two time constants, 4.6 ± 0.3 and 26.3 ± 1.0 ps, but a significant fraction of the excitations remain in B850 for considerably longer times. The fast step is interpreted as hopping of energy to LH1 from an associated LH2 complex; the slower steps are interpreted as migration of excitations in the LH2 pool preceding transfer to LH1. Transfer of excitations from B875 to B850 could not be detected, possibly suggesting that the average number of LH2 complexes in contact with each LH1 is small.

The antenna complexes of photosynthetic bacteria function to absorb light energy and transport it to the reaction center (RC)¹ where charge separation occurs. The antenna systems of the purple bacterium *Rhodobacter sphaeroides* and many related species consist of two major membrane-bound light-harvesting (LH) complexes, LH1 and LH2. The LH1 complex is believed to form a ring that surrounds the reaction center, while the smaller but more numerous LH2 complexes form a peripheral array (Papiz et al., 1996).

The crystal structure of the LH2 complex from *Rhodospseudomonas acidophila* has been determined to a resolution of 2.5 Å (McDermott et al., 1995; Freer et al., 1996). The complex has 9-fold rotational symmetry and contains nine copies each of two α -helical polypeptides (α and β), which form concentric cylinders with diameters of 36 and 68 Å, respectively. Sandwiched between the cylinders is a ring of 18 bacteriochlorophyll (BChl) molecules with their planes perpendicular to the membrane plane. Nine additional BChl molecules are bound to the β polypeptides in more isolated positions. At room temperature, the LH2 complex has two major near-infrared absorption bands at 850 and 800 nm. The 850 nm band is probably due to the ring of 18 BChls and the 800 nm band to the 9 additional molecules (Sauer et al., 1996; R. G. Alden et al., submitted for publication). For this reason, the two sets of pigments are known as B850 and B800. The LH2 complex of *Rhodospirillum rubrum* has a similar structure with 8-fold rotational symmetry (8 $\alpha\beta$ polypeptide heterodimers, 16 B850 BChls, and 8 B800 BChls) (Koepeke et al., 1996).

Electron-diffraction images of 2-dimensional arrays of the LH1 complex of *Rhodospirillum rubrum* reveal 16-fold

rotational symmetry (Karrasch et al., 1995). The 16 $\alpha\beta$ polypeptide heterodimers appear to form concentric cylinders with diameters of 68 and 116 Å and probably bind a ring of 32 BChl molecules. The LH1 complex has a near-IR absorption band that peaks at ~875 nm at room temperature; its pigments are termed B875. The center hole of the B875 complex is large enough to include an RC with its long axis normal to the membrane plane (Karrasch et al., 1995; Papiz et al., 1996).

Time-resolved absorption (Shreve et al., 1991; Hess et al., 1995; Wu et al., 1996) and fluorescence (Jimenez et al., 1996) studies of chromatophores and detergent-solubilized LH2 complexes have shown that energy transfer from the B800 BChls to the B850 ring occurs with a time constant of ~650 fs at room temperature. The transfer of energy from LH2 to LH1 has been reported to occur with multiphasic kinetics, including a component of <10 ps (Freiberg et al., 1989); Hess et al. (1995) give a time constant of ~3.3 ps. In the absence of energy transfer, the excited-state lifetimes of LH2 and LH1 embedded in the chromatophore membrane have been found to be 300 ± 50 and 335 ± 40 ps, respectively, at 77 K (Hunter et al., 1990).

In the present study, we explore the dynamics of energy transfer between LH1 and the B850 ring of LH2 in a mutant strain of *Rb. sphaeroides* that lacks the reaction center. Chromatophores are excited with weak, femtosecond pulses centered at 830 or 885 nm, and the resulting absorbance changes over the B850 and B875 absorption bands are analyzed globally.

MATERIALS AND METHODS

Rb. sphaeroides strains Δ QBALM/Q (Nagarajan et al., 1996), Δ RC-1A (Freiberg et al., 1996); and Δ LM1.1 (Paddock et al., 1989) were generously provided by Dr. J. C. Williams of Arizona State University. All three strains lack RCs; in addition, Δ RC-1A lacks LH2 and Δ QBALM/Q lacks LH1. Cells were grown and chromatophores isolated

[†] This work was supported by the Chemical Sciences Division of the U.S. Department of Energy (Contract FG06-94ER14443).

* Author to whom correspondence should be addressed.

[®] Abstract published in *Advance ACS Abstracts*, February 1, 1997.

¹ Abbreviations: BChl, bacteriochlorophyll; LH, light-harvesting (complex); RC, reaction center; SVD, singular-value decomposition.

and stored as described previously (Nagarajan et al., 1996). Chromatophore suspensions in 50 mM TRIS-HCl at pH 8.0 were filtered with a 220 nm pore-size membrane filter to remove aggregates and diluted to an absorbance of approximately 0.4–0.5 at 850 nm in a sealed quartz cuvette with a path length of 0.5 mm. During the experiment, the sample was refreshed continuously by translating the cuvette side-to-side at 1 cm/s.

The femtosecond spectrometer has been described in detail elsewhere (Nagarajan et al., 1996). Briefly, 12 fs wide pulses centered at 850 nm are produced by a mode-locked Ti:sapphire laser. The duty cycle of the pulses is reduced to 200 kHz with a Bragg cell. The pulses are split into pump and probe pulses with an intensity ratio of 9:1 and are sent down two different dispersion-precompensation lines. A movable slit of variable aperture placed near a collimating prism allows selection of both the central wavelength and the band width of the pump pulses. A chopper wheel modulates the pump beam at 1 kHz. The probe pulses are delayed by a computer-controlled delay stage, and the pump and the probe pulses are focused and crossed at the sample cuvette. The pump and probe pulses are polarized at 54.7° with respect to each other. Following the sample, the pump pulses are blocked and the probe pulses are detected with a photodiode after they have been passed through a monochromator with a 5 nm band width. The output of the photodiode is processed by a lock-in amplifier phase locked to the chopper frequency. Kinetic traces, collected at 5 nm wavelength intervals, are normalized to the DC level of the probe light and are subjected to singular-value decomposition (SVD) and global fitting to multiexponential functions as described previously (Nagarajan et al., 1993, 1996).

The cross correlation of the pump and the probe pulses is measured by focusing the pulses into a 30 μm thick KDP crystal, and the frequency-doubled light is detected with a photomultiplier. The width of the pump-probe cross correlation was typically 55 fs. At the combined irradiance of the pump and probe pulses at the sample ($\leq 1 \text{ W/cm}^2$), annihilation of excited singlet states by triplet states accumulated between pulses is a potential source of artifacts (Freiberg et al., 1989). However, the efficient quenching of BChl triplet states by carotenoids would make such artifacts relatively unimportant at the pulse repetition rate of the measurements (200 kHz).

RESULTS

The near-IR absorption spectrum of chromatophores from *Rb. sphaeroides* strain $\Delta\text{LM1.1}$ is shown in Figure 1A; Figure 1B shows absorption spectra of strains $\Delta\text{QBALM/Q}$ and $\Delta\text{RC-1A}$. The spectrum of strain $\Delta\text{LM1.1}$ (a strain that contains both LH1 and LH2) can be generated approximately, though not exactly, by a linear combination of the spectra of strains $\Delta\text{QBALM/Q}$ (LH2 only) and $\Delta\text{RC-1A}$ (LH1 only). Panel A of the figure also shows the spectra of excitation pulses tailored to excite preferentially either B850 (LH2) or B875 (LH1).

Figure 2A shows difference spectra measured 1 ps after excitation of $\Delta\text{QBALM/Q}$ chromatophores at 830 nm or excitation of $\Delta\text{RC-1A}$ chromatophores at 885 nm. These spectra provide signatures of excited states of B850 and B875, respectively. In the spectrum for B850, ground-state depletion and stimulated emission dominate at wavelengths

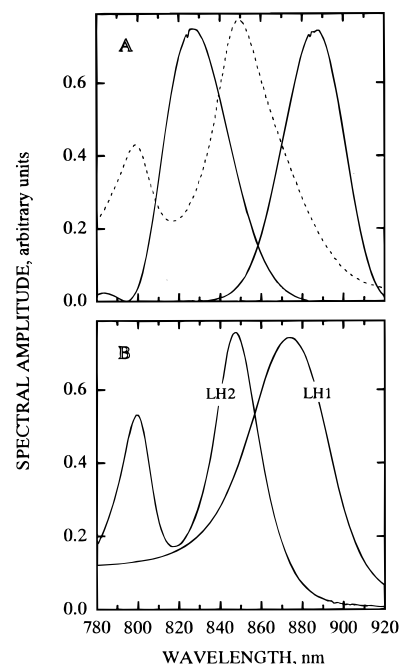


FIGURE 1: (A) Absorption spectrum of $\Delta\text{LM 1.1}$ chromatophores suspended in 50 mM TRIS-HCl at pH 8.0 (broken line) and intensity spectra of the pump pulses centered at 830 and 885 nm (continuous lines). (B) Absorption spectra of chromatophores of the strain $\Delta\text{QBALM/Q}$, which contains only LH2, and strain $\Delta\text{RC-1A}$, which contains only LH1.

longer than 845 nm and excited-state absorption dominates at shorter wavelengths. The spectrum for B875 has qualitatively similar features but is shifted about 30 nm to the red. Ground-state depletion and stimulated emission dominate at wavelengths to the red of 870 nm, and excited-state absorption dominates at shorter wavelengths. The excited-state absorption is somewhat broader than that associated with excitation of B850.

Because the absorption bands of the two complexes are not well resolved in the $\Delta\text{LM1.1}$ chromatophores, and the pump pulses produced as described in Materials and Methods have a large band width (Figure 1A), it is not possible to excite only one type of complex exclusively in this strain. However, since the amount of LH2 in the chromatophores considerably exceeds the amount of LH1, pulses centered at 830 nm are absorbed almost exclusively by B850. Pulses centered at 885 nm would excite predominantly B875, but a substantial fraction of B850 would also be excited.

Figure 3 shows difference spectra measured at several delay times following excitation of $\Delta\text{LM1.1}$ chromatophores with 830 nm pulses. The earliest spectrum is similar to the spectrum measured in strain $\Delta\text{QBALM/Q}$ (Figure 2A), displaying the characteristic features of excitation of B850. Between 0 and 50 ps, the signals in the 830 and 855 nm regions decay and a signal grows in at longer wavelengths. At longer times, there is an overall decay of the signal at all wavelengths and an apparent red shift of the signal at wavelengths longer than 880 nm.

The time-dependent spectra were analyzed by singular-value decomposition. Figure 4 shows the kinetic traces for the first four components of the analysis. The first three components clearly are significant, while the fourth cannot be distinguished from random noise. (Relative to the first component, the second, third, and fourth components had singular values of 10, 3, and 1%, respectively.) We therefore

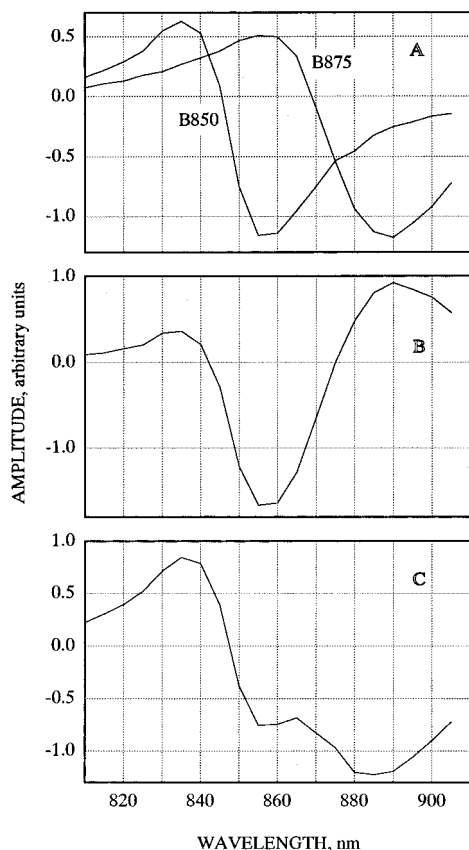


FIGURE 2: (A) Difference transmittance spectra at 1 ps following excitation of Δ QBALM/Q chromatophores at 830 nm (B850) and of Δ RC-1A chromatophores at 885 nm (B875). The spectra are normalized at the maximum of bleach. (B) Difference between the B850 and B875 spectra. (C) Sum of the B850 and B875 spectra after multiplying the B875 spectrum by 0.8.

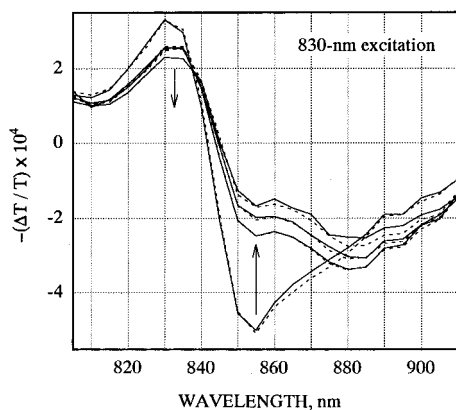


FIGURE 3: Representative difference transmittance spectra at 0, 50, 100, and 190 ps following excitation of Δ LM1.1 chromatophores with 830-nm pulses. Continuous lines are raw experimental data; broken lines, corresponding spectra reconstructed using the amplitude spectra and time constants given in the left panels of Figure 5. The arrows indicate the increasing time delay.

retained only the first three components for the next step of the analysis, in which the kinetics were fit globally to multiexponential functions. The smooth curves in Figure 4 show the results of fitting to a sum of three exponentials and a constant. The time constants of the exponential terms are 4.7, 25.8, and 103 ps. The left side of Figure 5 shows the amplitude spectra corresponding to these fits. The negative lobe near 850 nm in the amplitude spectra of the 4.7 and 25.8 ps components reflects a decay of the initial bleaching at this wavelength and the positive lobe at 830

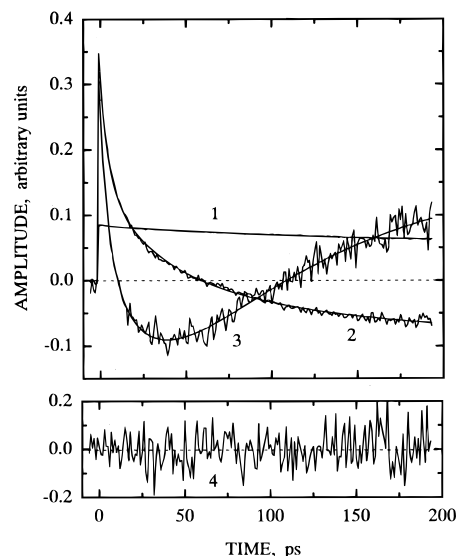


FIGURE 4: (Top) First three kinetics components from SVD analysis of difference spectra covering 200 time points and 22 wavelengths, obtained following 830 nm excitation of Δ LM1.1 chromatophores. The continuous lines are global fits to three exponentials and a constant. (Bottom) The fourth SVD component.

nm a decay of the excited-state absorption at short wavelengths, while the positive lobe in the 880–890 nm region reflects the growing in of bleaching and stimulated emission at longer wavelengths. The faster changes in the signals thus can be interpreted reasonably in terms of migration of excitations from B850 to B875.

The three dominant SVD components can also be fit to a sum of four exponentials and a constant, with slightly improved χ^2 values. The time constants returned by this fit are 4.8, 27.4, 96.6, and 143 ps. The corresponding amplitude spectra are shown on the right side of Figure 5. Again, the first two spectra appear to reflect energy transfer from B850 to B875; the third and fourth spectra appear to represent an arithmetic decomposition of the 103 ps amplitude spectrum on the left side of the figure. The time constants and the qualitative features of the amplitude spectra of the first two terms thus are relatively robust to the details of the kinetic analysis, although the relative amplitudes of the positive and negative lobes in the spectra are somewhat variable.

For comparison with the original experimental data, the dotted curves in Figure 3 show the data reconstructed from the amplitude spectra and the triexponential decay function. The excellent agreement between the original and reconstructed data out to at least 100 ps validates the SVD analysis and the global method of fitting the kinetics. The agreement between the experimental and reconstructed data at the longest time (190 ps) is less satisfactory, partly because of the inclusion of only the first three SVD components in the analysis. Although the components that were omitted had very small singular values and could not be distinguished from random noise, part of the signal could be distributed among a large number of minor components.

The measurements shown in Figures 3–5 were made with a time resolution of 1 ps and a total scan length of 200 ps. Analysis of spectra taken with a finer time resolution of 250 or 25 fs and scan lengths of 50 or 5 ps, respectively (not shown), revealed a ~ 4.5 ps component with an amplitude spectrum very similar in shape to that shown in the top panels of Figure 5. Additionally, fits of the higher-resolution data

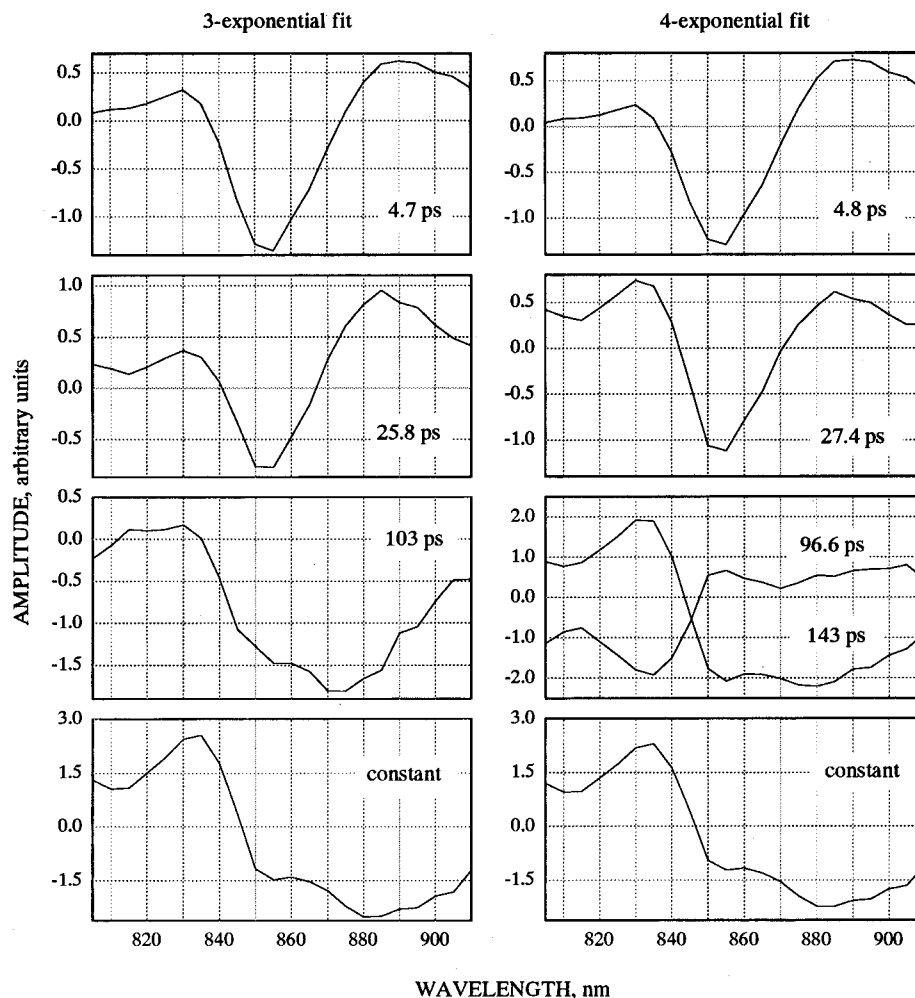


FIGURE 5: Amplitude spectra corresponding to the fits shown in Figure 4 (left panels) or to four exponentials and a constant (right panels). The corresponding time constants are given in each panel.

required an exponential term with a time constant of <300 fs. Because the broad-band 830 nm excitation (Figure 1) could also directly excite B800 to some extent, this ultrafast component could include energy transfer from B800 to B850 as well as the internal dynamics of B850 (Jimenez et al., 1996; Pullerits et al., 1996; Nagarajan et al., 1996). This component will not be discussed further here. The 50 ps data also revealed a 25 ps decay component with an amplitude spectrum similar in shape to that of the 25.8 or 27.4 ps components in Figure 5. Although the spectra of the 4.5 and 25 ps kinetic components measured with different time resolutions had minor variations in the relative amplitudes of the signals in the 830, 850, and 880-nm regions, they all had the same qualitative features, and in all cases the reconstructed total spectra resembled the experimental spectra closely.

To calculate the spectral changes that would be expected to accompany energy transfer from B850 to B875, the 1 ps difference spectrum measured with chromatophores of the mutant strain containing only LH1 (Δ RC-1A) was subtracted from the 1 ps difference spectrum measured following excitation of B850 in the strain containing only LH2 (Δ QBALM/Q). The calculated double-difference spectrum is shown in Figure 2B. Although the simulated spectrum is red shifted by ~ 5 nm, its shape is similar to that of the amplitude spectra in the top two panels of Figure 5. The spectrum of the "constant" term (bottom panels of Figure 5) can be attributed to a sum of excited B850 and B875, as

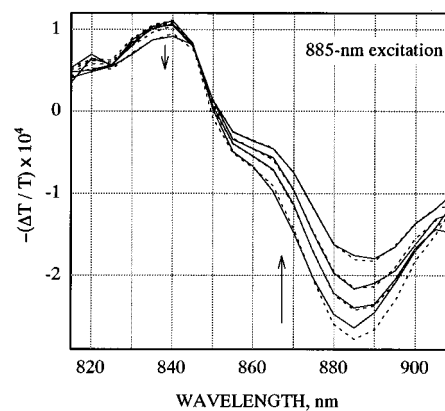


FIGURE 6: Representative difference transmittance spectra at 0, 50, 100, and 190 ps following excitation of Δ LM1.1 chromatophores with 885-nm pulses. Continuous lines are raw experimental data; broken lines are corresponding spectra reconstructed using the amplitude spectra and time constants given in Figure 8.

verified by its similarity to a simulated sum of the difference spectra of excited B850 and LH1 (Figure 2C). These simulations are not exact because, for reasons that are presently unclear, the B875 shoulder in strain Δ LM1.1 appears to be shifted slightly to the blue relative to the absorption band in strain Δ RC-1A.

Excitation of Δ LM1.1 chromatophores with pulses centered at 885 nm results in the spectra displayed in Figure 6. As discussed above, these pulses are expected to excite a

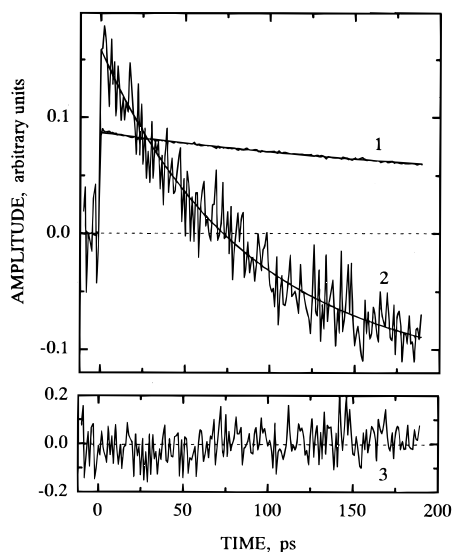


FIGURE 7: (Top) First two kinetics components from SVD analysis of difference spectra covering 200 time points and 20 wavelengths, obtained following 885 nm excitation of Δ LM1.1 chromatophores. The continuous lines are global fits to two exponentials (time constants of 75 and 200 ps) and a constant. (Bottom) The third SVD component.

certain fraction of B850 in addition to B875. The initial spectrum includes the ground-state bleaching and stimulated emission at long wavelengths expected for excited B875; the shoulder near 850 nm probably is attributable to B850 (*cf.* Figure 2A). Between 0 and 100 ps, there is a partial decay of the signal in the 860–885 nm range, and the signal throughout the spectrum continues to decay over the next 90 ps. There is a small red shift and broadening of the trough at 885 nm.

Singular-value decomposition of the data obtained with 885 nm excitation gave two significant components, which could be fit satisfactorily to the sum of two exponentials and a constant. Figure 7 shows the first three SVD kinetics components and fits to the first two; the third component seems to be mostly random noise. (Relative to the first component, the second and third had singular values of 4.7 and 2.4%, respectively.) The time constants returned by the global fit are 75 and 201 ps. The corresponding amplitude spectra are shown in Figure 8, and the reconstructed spectra are shown as dotted curves in Figure 6. The agreement with the raw experimental data is satisfactory, although the amplitude of the 0 ps spectrum is somewhat overestimated at long wavelengths. The two time constants are not sufficiently different and not sufficiently shorter than the time window of the experiment to make the fits unique; the results depend on the initial estimates of the parameters. (Another fit with a similar χ^2 had time constants of 105 and 132 ps. The amplitude spectra were qualitatively similar to those in Figure 8, but the trough at 870 nm in the spectrum of the faster component was less pronounced. A three-exponential fit returned an additional, very minor component with an amplitude spectrum resembling that of the constant component in Figure 8 and a time constant of 8 ps. However, χ^2 was not improved noticeably.)

Spectral components indicative of uphill energy transfer from B875 to B850 could not be resolved in the experiments performed with 885 nm excitation, possibly in part because the pulses generate a system in which distribution of

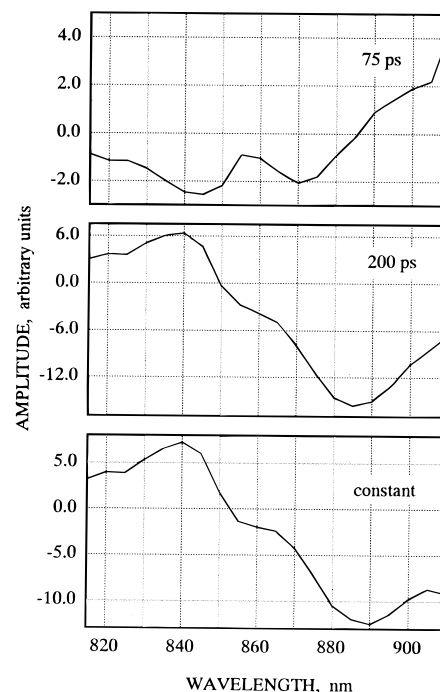


FIGURE 8: Amplitude spectra corresponding to the fits shown in Figure 7. The corresponding time constant is given in each panel. These fits are not unique (see the text).

excitations between the two complexes is close to equilibrium. However, complete equilibrium between excitations in LH1 and LH2 clearly is not attained within 200 ps after excitation with 830-nm pulses. The spectra measured at the longest times following excitation at 885 show considerably larger signals at 890 than at 855 nm (Figure 6), whereas those measured following excitation at 830 nm have similar amplitudes at these wavelengths (Figure 3). Examination of the amplitude spectra of the constant kinetic terms (bottom of panels of Figures 5 and 8) leads to the same conclusion. The difference between the two spectra measured 190 ps after excitation, after normalization at 885 nm, resembles the 0 ps spectrum of Figure 3, with an amplitude at 855 nm that is about 30% of the corresponding amplitude in the 0 ps spectrum. This suggests that approximately 30% of the excitations remain on B850 at ~ 200 ps.

DISCUSSION

As Figures 3–5 show, energy transfer to LH1 occurs in a multiphasic manner following excitation of B850 in LH2. In Figure 5, the amplitude spectra of the kinetic terms with time constants of 4.6 ± 0.3 (average value from three sets of data) and 26.3 ± 1.0 ps (average from two sets of data) are both qualitatively consistent with energy transfer from B850 to B875 (Figure 2B), and the spectrum of the constant term is consistent with a mixture of the excited states of B850 and B875 (Figure 2C). The 100 ps term has a distinctly different amplitude spectrum (Figure 5) and could include slow relaxations of the excited LH1 complex in addition to an overall decay of the excited states. Transients with time constants in the region of 100 ps and qualitatively similar spectra were seen when the chromatophores were excited at a wavelength that favors direct excitation of LH1 (Figure 8).

From fluorescence measurements with a time resolution on the order of 10 ps, Freiberg et al. (1989) concluded that

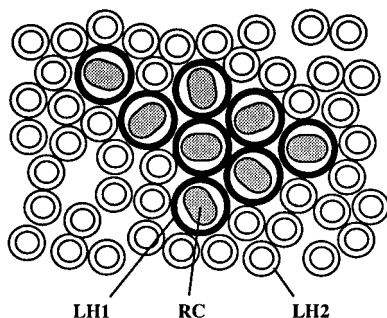


FIGURE 9: Plausible arrangement of LH1 and LH2 complexes in the chromatophore membrane.

energy transfer from B850 to B875 occurred in two stages with time constants of 8 and 25 ps and an $\sim 5:1$ amplitude ratio at room temperature. More recent pump-probe absorbance measurements by Hess et al. (1995) suggested a time constant of 3.3 ± 0.3 ps; however, these measurements were made at only three wavelengths and extended only to 4 ps after the excitation. The time constant of 4.5 ps that we measured is in the range of these earlier results, but probably is more reliable because we analyzed the spectra of B850 and B875 globally over their entire Q_y absorption band and measured the kinetics with adequate time resolution over several lifetimes of the major components.

Freiberg et al. (1989) assigned the biphasic kinetics to two distinct pools of B850 molecules that might be at different distances from B875. In light of the recent structural information (Karrasch et al., 1995; Koepke et al., 1996; Freer et al., 1996; Papiz et al., 1996), a straightforward interpretation is that the 4.5 ps step represents energy transfer directly to LH1 from attached LH2 complexes, and the 25 ps process reflects migration of excitations among LH2 complexes preceding transfer to LH1. A transfer or equilibration time constant of 4.5 ps seems consistent with direct Förster-type (dipole-dipole) energy transfer in a model in which an annulus of LH2 complexes surrounds LH1 (Hess et al., 1995; Papiz et al., 1996). At 855 nm, a wavelength diagnostic for B850, the fast decay term (Figure 5, top) has a relative amplitude of about 25%, compared to the amplitude of the initial bleaching (the sum of the amplitudes of all the exponential terms and the constant term). This suggests that on the order of 25% the initial excitations move directly to LH1. The slower kinetic terms could result from random walks of excitations among LH2 complexes that are not members of the immediate ring around LH1, with the constant term representing LH2 complexes that have no facile path to LH1. In this scheme, the observed time constant of 25 ps should be interpreted as an average value determined by fitting dispersive kinetics to a single exponential. The quality of the data does not allow us to distinguish between a single exponential and a continuous distribution of exponentials.

Figure 9 shows a model that is consistent with this analysis. The model is similar to one proposed earlier on the basis of measurements of singlet-triplet fusion (Monger & Parson, 1976), with the difference being that here one RC is associated with each LH1 complex. Because not all of the LH2 complexes are attached directly to an LH1, energy transfer from LH2 to LH1 would be multiphasic, as observed. This observation is more difficult to rationalize in the well-ordered model proposed by Papiz et al. (1996), in which each LH1 is surrounded by eight LH2 complexes and few if

any LH2 complexes reside in secondary rings or are free in the membrane. The model in Figure 9 also appears to be in better accord with the observation that the ratio of LH2 to LH1 in chromatophores varies strongly with culture conditions and can be as high as 11:1 in *Rb. sphaeroides* and 15:1 in *Rhodobacter capsulatus*. [These ratios were calculated from BChl:RC ratios summarized by Sistrom (1978), under the assumptions that LH1 and LH2 complexes contain 32 and 27 molecules of BChl, respectively, and each LH1 carries a reaction center. There is no indication that they are maximal ratios.]

An additional feature of the model shown in Figure 9 is a clustering of LH1-RC complexes in a domain surrounded by LH2s. This clustering was suggested by the singlet-triplet fusion studies (Monger & Parson, 1976). Because clustering of the LH1 complexes reduces the number of LH2 complexes in contact with each LH1, it could account for the fact that we did not detect energy transfer from LH1 to LH2 after excitation of $\Delta LM1.1$ chromatophores at 885 nm. The expected ratio of the two excited states for a system in quasi-equilibrium is given by

$$(B850^*):(B875^*) = R_s \exp(-\Delta E_{00}/k_B T) R_p \quad (1)$$

where R_s is the stoichiometric ratio of the two types of complex that communicate rapidly ($R_s = \text{LH2:LH1} = 8$ in the model proposed by Papiz et al. (1996)), ΔE_{00} is the difference between the 0-0 transition energies of the two complexes, k_B is the Boltzmann constant, T is the temperature, and R_p is the ratio of the partition functions of the excited complexes:

$$R_p = \left[\sum_i \exp(-\Delta E_i^{\text{LH2}}/k_B T) \right] / \left[\sum_i \exp(-\Delta E_i^{\text{LH1}}/k_B T) \right] \quad (2)$$

ΔE_i^{LH1} and ΔE_i^{LH2} are the energies of the i th excited level of the B875 and B850 rings, respectively, each measured from the lowermost excited level of the ring ($i = 1$). If we assume that the dispersions of the excited-state energies are similar in the two complexes, R_p is approximately the ratio of the number of exciton levels (or pigments) of B850 and B875, which is $18/32$ or 0.56 . This value probably is a lower limit considering that the width of the B875 absorption band is greater than that of B850 (approximately 650 versus 420 cm^{-1} ; see Figure 1B). From the absorption and emission maxima of purified LH2 and LH1 complexes at room temperature (Gottfried et al., 1991), the 0-0 transition energies are approximately $11\,710$ and $11\,250$ cm^{-1} , giving $\Delta E_{00} \approx 460$ cm^{-1} . The equilibrium $(B850^*):(B875^*)$ ratio in an $(\text{LH1})(\text{LH2})_8$ supercomplex thus should be on the order of 0.5 . If the 4.5 ps process that we observed following excitation at 830 nm represents an approach to this equilibrium from the direction of B850*, there should be a relaxation with a similar time constant following excitation of B875, with a relative amplitude of approximately 0.5 . This was not observed (Figure 7). However, as noted above, our results on this point are not definitive because the 885 nm excitation pulses are absorbed partly by LH2 in addition to LH1.

Additional evidence that the rate of return of excitations from LH1 to LH2 is slower than might be expected if each LH1 were in contact with eight LH2 complexes has come from studies of "delayed" emission. Delayed emission is seen subsequent to the excitation of chromatophores in which

a secondary electron transfer step is blocked and reflects the return of excitations to the antenna after charge recombination within the RC. The measured spectrum of delayed emission from *Rb. sphaeroides* chromatophores is dominated by B875 with a small ($\leq 5\%$) contribution from B850 (Woodbury & Parson, 1986). By contrast, the spectrum of the "prompt" fluorescence emitted while excitations are moving from the antenna to the RCs is dominated by B850. Our results appear to be consistent with these findings.

It is possible that the very slow transfer of a portion of the excitations to LH1 results from preparation of a heterogeneous population of membrane fragments, some of which contain LH2 complexes but lack LH1. Our measurements therefore do not necessarily pertain closely to the structure of the antenna in intact cells. It also is possible that the slow transfer is peculiar to the mutant strain we used. Fluorescence decay components exceeding 100 ps were not seen by Freiberg et al. (1989) in wild-type cells or chromatophores, as long as a reductant was added to keep the RC in a photochemically active state. Hunter et al. (1990) have emphasized that mutations that remove major membrane complexes such as the RC could have pleiotropic effects, possibly including changes in the association between antenna complexes. In wild-type strains, a larger fraction of the LH2 complexes might be bound directly and aggregates of LH1 might be rarer than suggested by the model in Figure 9.

ACKNOWLEDGMENT

We are grateful to JoAnn Williams for providing cells and cultures of the mutant strains and to Rhett Alden and Paula Johnson for their help with growing the cells. We also thank Rhett Alden for helpful discussions.

REFERENCES

- Bradforth, S. E., Jimenez, R., van Mourik, F., van Grondelle, R., & Fleming, G. R. (1995) *J. Phys. Chem.* 99, 16179–16191.
- Freer, A., Prince, S., Sauer, K., Papiz, M., Hawthornthwaite-Lawless, A., McDermott, G., Cogdell, R., & Isaacs, N. W. (1996) *Structure* 4, 449–462.
- Freiberg, A., Godik, V. I., Pullerits, T., & Timpman, K. (1989) *Biochim. Biophys. Acta* 973, 93–104.
- Freiberg, A., Allen, J. P., Williams, J. C., & Woodbury, N. W. (1996) *Photosynth. Res.* 48, 309–319.
- Gottfried, D. S., Stoker, J. W., & Boxer, S. G. (1991) *Biochim. Biophys. Acta* 1059, 63–75.
- Hess, S., Chachisvilis, M., Timpmann, K., Jones, M. R., Fowler, G. J. S., Hunter, C. N., & Sundström, V. (1995) *Proc. Natl. Acad. Sci. U.S.A.* 92, 12333–12337.
- Hunter, C. N., Bergström, H., van Grondelle, R., & Sundström, V. (1990) *Biochemistry* 29, 3203–3207.
- Jimenez, R., Dikshit, S. N., Bradforth, S. E., & Fleming, G. R. (1996) *J. Phys. Chem.* 100, 6825–6834.
- Karrasch, S., Bullough, P. A., & Ghosh, R. (1995) *EMBO J.* 14, 631–638.
- Koepeke, J., Hu, X., Muenke, C., Schulten, K., & Michel, H. (1996) *Structure* 4, 581–597.
- McDermott, G., Prince, S. M., Freer, A. A., Hawthornthwaite-Lawless, A. M., Papiz, M. Z., Cogdell, R. J., & Isaacs, N. W. (1995) *Nature* 374, 517–521.
- Monger, T. G., & Parson, W. W. (1976) *Biochim. Biophys. Acta* 460, 393–407.
- Nagarajan, V., Parson, W. W., Davis, D., & Schenck, C. C. (1993) *Biochemistry* 32, 12324–12336.
- Nagarajan, V., Alden, R. G., Williams, J. C., & Parson, W. W. (1996) *Proc. Natl. Acad. Sci. U.S.A.* 93, 13774–13779.
- Paddock, M. L., Rongey, S. H., Feher, G., & Okamura, M. Y. (1989) *Proc. Natl. Acad. Sci. U.S.A.* 86, 6602–6606.
- Papiz, M. Z., Prince, S. M., Hawthornthwaite-Lawless, A. M., McDermott, G., Freer, A. A., Isaacs, N. W., & Cogdell, R. J. (1996) *Trends Plant Sci.* 1, 198–206.
- Pullerits, T., Chachisvilis, M., & Sundström, V. (1996) *J. Phys. Chem.* 100, 10787–10792.
- Reddy, N. R. S., Picorel, R., & Small, G. J. (1992) *J. Phys. Chem.* 96, 6458–6464.
- Sauer, K., Cogdell, R. J., Prince, S. M., Freer, A. A., Isaacs, N. W., & Scheer, H. (1996) *Photochem. Photobiol.* 64, 564–576.
- Schreve, A. P., Trautman, J. K., Frank, H. A., Owens, T. G., & Albrecht, A. C. (1991) *Biochim. Biophys. Acta* 1058, 280–288.
- Sistrom, W. R. (1978) in *The Photosynthetic Bacteria* (Clayton, R. K. & Sistrom, W. R., Eds.) pp 841–848, Plenum, New York.
- Woodbury, N. W., & Parson, W. W. (1986) *Biochim. Biophys. Acta* 850, 197–210.
- Wu, H.-M., Savikhin, S., Reddy, N. R. S., Jankowiak, R., Cogdell, R., Struve, W. S., & Small, G. J. (1996) *J. Phys. Chem.* 100, 12022–12033.

BI962534B